SOLVING THE NONLINEAR PENDULUM EQUATION WITH FRICTION AND DRAG FORCES USING THE FINITE ELEMENT METHOD

YOUSSEF I. HAFEZ

Abstract. Pendulum phenomenon plays an important, role in applied mathematics, earthquake engineering, vibrations mechanics and physics due to its dynamical nonlinear nature. The nonlinear pendulum governing differential-equation is numerically solved herein using the Finite Element Method for the first time. To overcome the nonlinearity resulting from the sine term, Maclaurin's power-series expansion for the sine function with ten terms (odd powers up to the 19th power) is substituted into the differential equation. The nonlinearity is then shifted from the sine term to terms of powers of the angular displacement. The original initial value pendulum problem is converted into a two-point boundary value problem suitable for the Finite Element Method. This is possible owing to a power series solution that determines an explicit expression of the period of motion in terms of the initial displacement angle (amplitude). In this way the time of motion which is given by the period of motion is considered as a space domain. The periodic nature of the pendulum problem allows specifying the amplitude value at the two ends of the time domain (now becomes the space domain) as the two end boundary conditions. An incremental boundary condition technique and the Newton-Raphson method are used to solve the nonlinear system of equations. The solution is applicable up to maximum amplitude of 179º. The differential form of the pendulum equation facilities investigating damped motion by including the frictional and form drag resistance forces to the differential equation of the pendulum motion in fluids such as air and water. The ability to solve the differential equation form of the nonlinear pendulum allows ease in dealing with tangential forces to the pendulum bob's direction of motion such as fluid resistance and electromagnetic forces. Comparison with existing analytical solution shows that the present approach succeeded in predicting the pendulum motion profile under damped conditions. The approach developed here could be used to investigate pendulum problems where electromagnetic forces exist.

Key words: nonlinear pendulum, damped oscillations, Galerkin's finite element method, maclaurin's power series, incremental boundary conditions technique, friction and form drag resistance forces.

1. INTRODUCTION

Pendulum phenomenon plays a very important role in applied mathematics, earthquake engineering, vibrations mechanics and physics due to its dynamical

Nile Research Institute, Cairo, Egypt

Ro. J. Techn. Sci. – Appl. Mechanics, Vol. 67, N° 2, P. 137–161, Bucharest, 2022

nonlinear nature. The simple pendulum is an idealized dynamical nonlinear model for the real pendulum. It is consisting of a rod of length *L* and a bob of mass m with a rod/string/cable that is not extensible, and its weight is negligible [1]. For the undamped pendulum it is assumed that there is no loss of energy and no friction.

By applying Newton's second law of motion to the forces acting on the bob in the tangential direction of motion, we have the following second-order nonlinear differential equation

$$\theta''(t)+\frac{g}{L}\sin\theta(t)=0\,, \tag{1}$$

where θ" (t) is the second time derivative of θ(t) or the angular acceleration, θ(t) is the angular displacement of the bob measured from the vertical line in a counterclockwise direction as a function of time, t, and g is the gravitational acceleration. Two boundary conditions are associated with Eq. (1) namely $\theta(0)=\theta_0$ and θ'(0) = 0 where θ_0 is the amplitude of the oscillation or the maximal angular displacement or the initial displacement angle. The angle is considered positive for counterclockwise rotation and vice versa. The maximum displacement angle considered is θ < ±180° or specifically herein it is taken as ±179°. In real life one can see in amusement parks swings with maximum displacement angles approaching ±179° when no full swings are allowed while in other cases full swings might be possible with θ reaches up to 360°.

When θ is small (θ < 15°), sin θ can be approximated by θ [2]. This gives the linearized model:

$$\theta''(t)+\frac{g}{L}\theta(t)=0 \tag{2}$$

.

The general solution for Eq. (2) is given by

$$\theta''(t)=\theta_0\cos\left(\left(\sqrt{\frac{g}{L}}\right)t\right). \tag{3}$$

We assume that $0 < \theta_0 < \pi$ such that the pendulum does not go around the pivot and bob is never directly above the pivot. From now on and for convenience the symbol θ will be used instead of θ (*t*).

From the law of conservation of energy, we get:

$$E=mgL\left(1-\cos\theta_o\right)=\frac{1}{2}mL^2\left(\frac{\mathrm{d}\theta}{\mathrm{d}t}\right)^2+mgL(1-\cos\theta), \tag{4}$$

where *E* is the total energy of the pendulum system, the first term on the right hand side is the kinetic energy and the second term is the potential energy. Eq. (4) can be written as:

$$\frac{\mathrm{d}\theta}{\mathrm{d}t} = \pm\sqrt{\frac{2g}{L}}\sqrt{\left(\cos\theta - \cos\theta_0\right)}, \tag{5}$$

where + (–) sign is for counter-clockwise (clockwise) motion. By integrating $\frac{\mathrm{d}\theta}{\mathrm{d}t}$ in Eq. (5), the exact period T can be calculated from the expression:

$$T = 4\sqrt{\frac{L}{g}}\int_0^{\pi/2}\frac{1}{\sqrt{(1-k^2\sin^2\varphi)}}\,\mathrm{d}\varphi, \tag{6}$$

where $k = \sin\left(\theta_0/2\right)$. The definite integral in Eq. (6) is the complete elliptic integral of the first kind which was used often a lot for analyzing the nonlinear pendulum motion.

[3], [4] gave the power series solution to the pendulum equation, Eq. (6), as follows:

$$T = T_0\left[1+\left(\frac{1}{2}\right)^2 k^2 + \left(\frac{1.3}{2.4}\right)^2 k^4 + \left(\frac{1.3.5}{2.4.6}\right)^2 k^6 + \ldots\right], \tag{7}$$

where $T_0 = 2\pi\sqrt{\frac{L}{g}}$ is the period of the linear pendulum equation which was given in Eq. (2).

Reference [5] presented exact formulas for the period and angular displacement of the nonlinear pendulum as a function of: the time, the amplitude of oscillations and the angular frequency for small oscillations. This angular displacement was written in terms of the Jacobi elliptic function sn(u;n). The angular displacement is plotted using Mathematica computer program.

Reference [6] presented an analytical solution for the differential equation of the simple nonlinear pendulum based on Jacobi elliptic functions. He presented analytically and graphically the angle and angular velocity for amplitudes up to 179.9°.

Reference [7] used the exact expression for the maximum tension of a pendulum string to obtain a closed-form approximate expression for the solution of nonlinear simple pendulum in terms of elementary functions (cosines functions). Their developed scheme gave excellent approximations for amplitudes as high as 170°.

Reference [1] using numerical investigation in the form of Gaussian quadrature technique which was applied to the elliptic integral equation of the first kind, presented complete analysis of the period, profile motion, velocity, potential energy and kinetic energy of the nonlinear pendulum. In addition, an expression was presented to calculate the gravitational acceleration for amplitudes in the range given by $0 < \theta_0 < \pi/2$. For amplitudes greater than 170°, the angle profile was not smooth as it should be due to approaching singularity of the integral equation in the proximity of 180°.

Reference [8] performed Fourier series analysis of a pendulum undergoing large-scale oscillation (but maximum amplitude was 1.7 rad = 97.4°) without going into the involved mathematics of elliptic integrals and Jacobi elliptic functions which compose the exact solution of the pendulum nonlinear differential equation.

The forgoing brief literature review points out previous studies are mostly based on the elliptic integral equation of the first kind and the complex Jacobi elliptic functions through complex analytical functions. The energy formulation of the pendulum, Eq. (5), was the starting point in all of these analyses. The developed approach herein is based on balance of forces and differs from previous approaches which used the energy balance formulation. In the previous approaches full utilization was not made of the power of computer computational technology and the well-known numerical methods such as the Finite Element Method (FEM) and Finite Differences which have been used successfully to solve other differential equations. The differential equation formulation of the pendulum offers ease in handling forces other than gravitational forces such as frictional/ dissipative and electromagnetic driving forces. Other more complex types of pendulums such as: the spring, double and coupled pendulums could be investigated at high oscillations when utilizing the power of numerical methods.

Because the differential equation and boundary conditions of the simple nonlinear pendulum constitutes an initial value problem (IVP), FEM could not be applied directly as it is suited for boundary values problems (BVP). This is due to the fact that in the FEM the space coordinates are the one to be discretized. The way to overcome this difficulty and to overcome the high nonlinearity inherited of the pendulum differential equation is presented hereinafter.

2. METHODOLOGY FOR UNDAMPED OSCILLATIONS

The objective of this study is to give a new approximating form to the pendulum governing differential equation. The complex nonlinearity of this equation stems from the fact that the unknown function (the angular displacement) appears inside the sine function as seen in Eq. (1). Adding frictional and electromagnetic forces render the pendulum equation very difficult for an analytical solution to be reached. This problem caused well-known numerical methods such as Finite differences and Finite Elements to avoid tackling the nonlinear pendulum problem. The complex nonlinearity of the pendulum D.E. is overcome through the removal of the term sinθ by utilizing the Maclaurin's power series expansion for sin θ which is given as:

$$\sin\theta = \sum_{n=0}^{\infty} (-1)^n \frac{\theta^{2n+1}}{(2n+1)!}, \tag{8}$$

where θ is in radians. Substituting Eq. (8) into Eq. (1) yields:

$$\theta''(t)+\frac{g}{L}\sum_{n=0}^{\infty}(-1)^n\frac{\theta^{2n+1}}{(2n+1)!}=0\,. \tag{9}$$

In Eq. (9) the non-linearity is shifted from the sine term into powers of the angular displacement of the pendulum bob. The expanded form of Eq. (9) considering for example 10 terms in the Maclaurin's power series is:

$$\theta''(t)+\frac{g}{L}\left(\theta-\frac{\theta^3}{3!}+\frac{\theta^5}{5!}-\frac{\theta^7}{7!}+\frac{\theta^9}{9!}-\frac{\theta^{11}}{11!}+\frac{\theta^{13}}{13!}-\frac{\theta^{15}}{15!}+\frac{\theta^{17}}{17!}-\frac{\theta^{19}}{19!}\right)=0 \tag{10}$$

Conventional approximating functions such as those given by Finite Differences and Finite Element methods can now be substituted for θ in Eq. (10). Now the floor is open to apply numerical methods to solve Eq. (10) as the angular displacement can be approximated by a piece-wise linear function as often done in the context of FEM. However, the FEM is suited to boundary values problems. The simple nonlinear pendulum in Eq. (10) is, however, an initial value problem. By treating the time domain as a space domain, the period of the amplitude of the pendulum can be considered as the length of the domain. In other words the length of the domain is taken equal to the period T which can be computed from Eq. (7) for every specific θ_0 value. The boundary conditions for Eq. (1) could be:

$$\theta(0)=\theta_0 \text{ and } \theta(T)=\theta_0\,, \tag{11a}$$

$$\text{or } \theta(0)=\theta_0 \text{ and } \dot{\theta}(T)=\theta_0\,. \tag{11b}$$

The periodic nature of the pendulum problem allows imposing boundary conditions in the form given by Eq. (11a and b). However, as will be seen later, Eq. (11b) as a boundary condition can be used in which the velocity at the end of the period is taken as zero. The boundary conditions in Eq. (11) convert the IVP to a two-point BVP suitable for treatment by the FEM.

3. THE FEM NUMERICAL MODEL STRUCTURE

The space domain of length equal to the period *T* is divided into a number of elements of equal lengths. Over each element the unknown function (angular displacement θ) is approximated by a linear function, [9], as by:

$$\theta(x)=\Theta_L+(\Theta_R-\Theta_L)\left(\frac{x}{l_e}\right), \tag{12}$$

where $\theta(x)$ is the value of θ inside the element, Θ_L is the value of θ at the left end of the element (nodal value), Θ_R is the value of θ at the right end of the element (nodal value) and l_e is the element length. Note the space coordinate *x* is actually representing the time *t*.

The Galerkin Finite Element Method, [9], starts by multiplying the governing differential equation by a suitable weighting function (which is an infinitesimal variation of θ, i.e. δθ) and integrating over each element length. The governing equation thus becomes an integral differential equation. Integration by parts reduces the second order derivative term one order less, i.e. to a first derivative, allowing the substitution of the linear approximating function as given in Eq. (12). This process converts the integral differential equation into integral algebraic equation which can be written in matrix form. An element matrix is associated with the first term in Eq. (1), which now has a first derivative, and another element matrix is associated with the θ term in Eq. (1). Integration of the element matrices is performed using Gaussian quadrature technique. The element matrices are then assembled into the global matrix equation which for nonlinear problems like the pendulum problem at hand has the form:

$$\left[K(\theta)\right]\{\theta\} = \{Q\}, \tag{13}$$

where $[K(\theta)]$ is the stiffness matrix of the system which is a nonlinear matrix, $\{\theta\}$ is the unknown solution vector and $\{Q\}$ is the forcing-function vector. The forcing function vector has zero values at all the nodes except at the boundary points to enforce the boundary conditions given in Eq. (11). Equation (13) can be solved by the method of successive iterations, but its convergence would be slow as it is linear, [10]. To speed up the convergence to quadratic convergence, [10], the Newton-Raphson method for nonlinear equation systems is used. This is done by transforming Eq. (13) into the following equation:

$$\left[JK(\theta)\right]\{\Delta\theta\} = \{Q\} - \left[K(\theta)\right]\{\theta\}, \tag{14}$$

where $\left[JK(\theta)\right] = \left[\frac{\partial}{\partial\theta}\left(K(\theta)\right)\right]$ is the Jacobian matrix for nonlinear systems and $\{\Delta\theta\}$ is the increment or correction vector of $\{\theta\}$. The solution vector $\{\theta\}$ at iteration $n+1$ is obtained as

$$\{\theta\}^{n+1} = \{\theta\}^n + \{\Delta\theta\}^n, \tag{15}$$

where *n* is the iteration number. In the first iteration upon solving Eq. (14), the unknown solution-vector $\{\theta\}$ is assumed with suitable initial values which are then updated *via* Eq. (15) in the next iteration and so on until the maximum absolute difference between two successive iterations at any node is within a specified

tolerance. This process is performed for every specific amplitude or initial angular displacement, θ_0. A non-symmetric banded equation solver is used to solve the resulting system of algebraic equations. The existence of frictional forces, where the non-symmetric operator derivative of θ exists, requires using non-symmetric banded matrix storage form. As the system of equations is similar to problems that are one-dimensional in which the band width is three, the resulting banded matrix would have the dimension of *N* by 3, where *N* is the number of equations which is equal to the number of elements increased by one. Because the system matrix is banded and its band width is only equal to three, large system of equations in the order of thousands can be handled easily. A Computer program in FORTRAN programming language was developed to implement the above solution procedure of the nonlinear pendulum equation using the FEM.

To overcome the high nonlinearity of the governing equation, it is required that a good initial or trial solution is substituted in the left and right hand side of Eq. (14). In other words, the trial or guessed initial solution values must be close to the final solution to ensure speedy convergence of the solution process. The initial angular displacement, θ_0 constitute the essential boundary conditions at the two end-points of the domain when using Eq. (11a). Initially θ_0 is assumed equal to 1º then Eq. (14) is solved iteratively till the maximum absolute difference of the angular displacement (in radians) at all nodes between each two successive iterations is less than a tolerance which was taken equal to 10^{-7}. Maximum number of iterations is set equal to 100 while convergence took usually few-iterations. This means attaining convergence for a value of θ_0 equal to 1°. Then θ_0 is increased by one more degree (and a new period is computed from Eq. (7)) and the solution from the old or last θ_o is used as the initial guess for the new θ_0.

The process of increasing θ_0 by one degree increments is continued until the required actual boundary condition value of θ_0 is attained. The maximum value of θ_0 is 179°. The procedure just described is the incremental boundary condition technique developed herein to obtain a good trial or guessed initial solutions for specific amplitude.

Now for the specific amplitude under consideration, another iteration cycle is performed (for the given θ_0). The computed total energy (sum of potential and kinetic energy in the right hand side of Eq. (4)) is calculated at all nodes. A central difference is used for the derivative $\frac{\mathrm{d}\theta}{\mathrm{d}t}$ at all interior nodes as follows:

$$\left(\frac{\mathrm{d}\theta}{\mathrm{d}t}\right)i = \frac{\theta_{i+1} - \theta_{i-1}}{2l_e}. \tag{16}$$

The exact total energy is already known as from the left hand side of Eq. (4) as $E = mgL\ (1-\cos\theta_0)$. When the maximum relative absolute difference between the exact energy of the system and the computed energy as a percentage is less than 0.02%, convergence can be assumed and the iteration process is stopped. The maximum possible number of iterations was set equal to 1 000. At final convergence, the resulting FEM solution satisfies both convergence of θ and convergence of the computed energy to the actual energy. The resulting solution would be the final computed solution by the FEM to the nonlinear pendulum equation Eq. (1).

4. NUMERICAL DETAILS OF THE FEM MODEL

The most critical case is that for amplitude of 179°. It is discussed in detail herein first due to its challenging nature because it is in the super high regime $\left(\theta > 150^0\right)$ which was defined in [1]. The period for the 179° amplitude was computed from Eq. (7) to be 7.8061 s. This value was taken equal to the length of the domain which is divided into a number of elements. To decide on the appropriate number of elements several numerical runs were implemented taking different number of elements as seen in Table 1.

Table 1

Effect of number of elements

Number of elements	Relative error in energy [%]	Total number of iterations
100	1.94261	1 409
200	0.49470	1 418
500	0.07955	1 555
1 000	0.01991	659
2 000	0.00497	937
3 000	0.00557	1 676
4 000	0.00540	2 117

For the case of having 100 elements, the error in energy, Table 1, was about 1.94% and took 1 409 iterations to reach. In the process of incremental increase of the initial amplitude from 1° until reaching the 178° amplitude and at any amplitude inside that range it took mostly from 3 to 5 iterations to reach a tolerance of 10^{-7} in θ. When the amplitude became 179° it took 8 iterations to satisfy that tolerance. The number of iterations up to that extent reached 409 but the tolerance in energy was not satisfied (error in energy chosen to be less than 0.02%). The model was run for extra 1 000 iterations keeping the amplitude as 179° but that was not enough to satisfy the energy tolerance although the tolerance of θ was in the

order of 10^{-9}. For the 200 and 500 elements the same situation occurred, i.e. not satisfying the energy tolerance. For 200 elements it took 16 iterations at amplitude of 179° for convergence in θ. For 500 elements, different odd behavior was there as 60 iterations at amplitude of 118° and 20 iterations at amplitude of 168º were needed for convergence in θ.

For 1000 elements the total number of iterations was only 659. At amplitude of 179°, 16 iterations were needed for convergence in θ as seen in Table 2 and at that point the number of iterations reached 658. After 16 iterations at 179° amplitude, it took an extra one iteration to satisfy the energy tolerance while the error in θ was 7.0×10^{-9}. For the 2 000, 3 000 and 4 000 elements, significant number of iterations at the intermediate amplitudes in the order of 20 to 30 iterations caused the total number of iterations to be relatively higher but the energy error decreased significantly. The error history at 1 000 elements is quite normal as seen in Table 2, with few iterations required before reaching the 179° amplitude. Therefore, 1 000 elements were considered throughout the remaining of the study for one rotational cycle. For two rotational cycles (the domain length is equal to two periods) 2 000 elements were found sufficient and the energy error reached 0.01988%.

Table 2

Number of iterations and absolute differences in θ for different amplitudes for 1 000 elements

Amplitude in Degrees	Number of Iterations	Absolute Maximum Difference in θ (radians) between two successive iterations
169	1	0.0329000000
169	2	0.0004790000
169	3	0.0000089000
169	4	**0.0000000254**
170	1	0.0349000000
170	2	0.0005090000
170	3	0.0000119000
170	4	0.0000001030
170	5	**0.0000000589**
171	1	0.0374000000
171	2	0.0005540000
171	3	0.0000169000
171	4	**0.0000000172**
172	1	0.0405000000
172	2	0.0006190000
172	3	0.0000256000
172	4	**0.0000000901**
173	1	0.0443000000
173	2	0.0007280000
173	3	0.0000455000

173	4	**0.0000000225**
174	1	0.0493000000
174	2	0.0009130000
174	3	0.0000995000
174	4	**0.0000000316**
175	1	0.0560000000
175	2	0.0013300000
175	3	0.0003330000
175	4	0.0000001540
175	5	**0.0000000271**
176	1	0.0654000000
176	2	0.0071600000
176	3	0.0063200000
176	4	0.0000668000
176	5	0.0000003310
176	6	**0.0000000449**
177	1	0.0800000000
177	2	0.0023600000
177	3	0.0026300000
177	4	0.0000025000
177	5	**0.0000000078**
178	1	0.1050000000
178	2	0.0032700000
178	3	0.0047600000
178	4	0.0000172000
178	5	0.0000001770
178	6	**0.0000000388**
179	1	0.1640000000
179	2	0.0074800000
179	3	0.0267000000
179	4	0.0136000000
179	5	0.0271000000
179	6	0.0304000000
179	7	0.0675000000
179	8	0.0166000000
179	9	0.1930000000
179	10	0.0053400000
179	11	0.0810000000
179	12	0.0015900000
179	13	0.0117000000
179	14	0.0000905000
179	15	0.0000210000
179	16	**0.0000000426**
180	1	**0.0000000070**

Figure 1 shows the errors history when using 1 000 elements. It is clear that for amplitudes up to 98°, three iterations were sufficient for the absolute difference in θ between successive iterations to be less than the tolerance value of 10^{-7}. Eight, eleven, twelve and sixteen iterations were needed at high amplitudes of 117°, 138°, 152° and 179°, respectively. Table 2 sheds more light by showing the number of required iterations and the associated maximum absolute difference (shown in red color at convergence) in θ starting at amplitude 169° up to 179°. Interestingly the number of iterations increases significantly to 16 at the amplitude of 179°. This means that the FEM solution has converged in its nonlinear phase as the maximum absolute difference in θ, between any two successive iterations, is less than 10^{-7} but this does not mean necessarily that the maximum error in energy is less than the energy tolerance (0.02%). It took one iteration cycle to attain an error of energy as low as 0.01991%. Now the obtained numerical solution satisfies both error tolerances in the calculated θ and in the calculated energy. It should be noted that 9 Gaussian quadrature points and 10 terms of the Maclaurin's series for sin θ were considered in the foregoing numerical runs. To investigate numerical integration, four, seven and nine Gauss quadrature points were tried upon to integrate the element matrices while using 1000 elements and 10 terms of the Maclaurin series for sin θ.

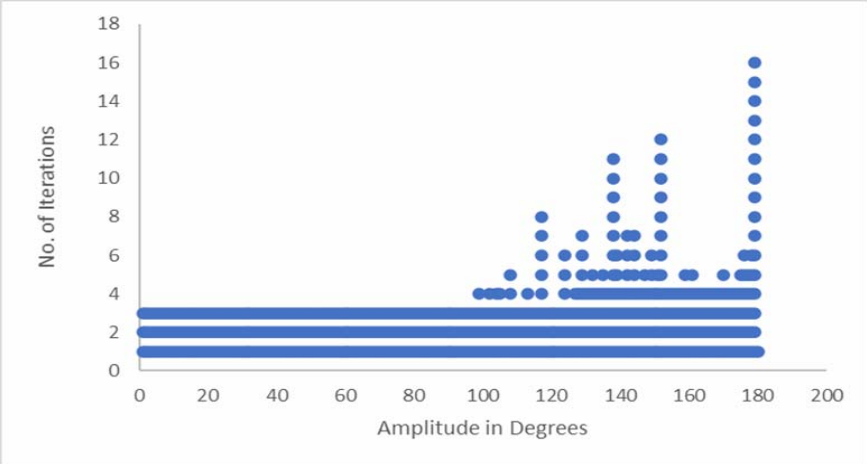

Fig. 1 – Number of iterations for convergence at each trial amplitude angle.

Table 3 shows that no significant difference is there between the three types of the Gaussian quadrature points with the 9 points having the least number of iterations. If the integrand can be approximated by a polynomial, using nine points integrates that polynomial exactly up to the 17^{th} power. Therefore, 9 Gaussian quadrature points were selected to give the best possible accuracy in the numerical integration.

Table 3

Effects of the number of Gaussian quadrature points

Number of Quadrature Points	Relative Error in Energy [%]	Number of Iterations
4	0.01991	676
7	0.01991	679
9	0.01991	659

Table 4 shows the effects of using different number of terms of the Maclaurin series for sin θ while using 1 000 elements and 9 Gaussian quadrature points. It is apparent that starting from 7 terms of the Maclaurin series for sin θ and higher the required accuracy in energy calculations is attained. As seen from Table 4, adding more terms in Maclaurin's series reduces the energy errors. Convergence was not possible when using three terms for reasons to be found is beyond the scope of this study.

Table 4

Effects of number of terms in Maclaurin series

Number of Terms in Maclaurin Series	Relative Error in Energy [%]	Number of Required Iterations
1	174.8	1 179
2	26.96	1 413
3	Divergence	-------
4	0.09143	1 865
5	0.10210	1 574
6	0.02452	1 445
7	0.01452	694
8	0.01991	655
9	0.01991	679
10	0.01991	659

Based on the foregoing numerical analyses, it can be concluded that choosing a combination of 1 000 elements, nine Gaussian quadrature points and 10 terms of the Maclaurin power series would be sufficient in obtaining accurate FEM numerical solutions that satisfy both tolerances in convergence of the angular displacement (θ) and the energy for all the considered range of amplitudes. Therefore, these choices or parameters will be adopted in all the numerical runs that will follow. The intention here is not to seek the minimum or necessary requirements for these parameters but is to select sufficient choices in order to cover all possible situations or applications especially when including frictional forces later. Table 5 shows the energy errors using these parameters for some selected amplitudes that cover a wide range of the pendulum motion. As expected the lesser the initial displacement angle or amplitude the lesser the energy error would be due to a decreased level in nonlinearity. Now the numerical results are presented for some selected amplitudes.

Table 5

Errors in energy at different amplitudes

Amplitude in Degrees	Relative Error in Energy [%]
14	0.00165
30	0.00168
60	0.00180
75	0.00191
90	0.00206
135	0.00318
150	0.00415
160	0.00534
170	0.00784
179	0.01991

5. RESULTS OF THE FEM NUMERICAL MODEL

Figure 2 shows the FEM computed motion profile of θ with time for one cycle at amplitude of 179° using the boundary conditions as in Eq. (11a). This profile is conforming to that of [5] and [6].

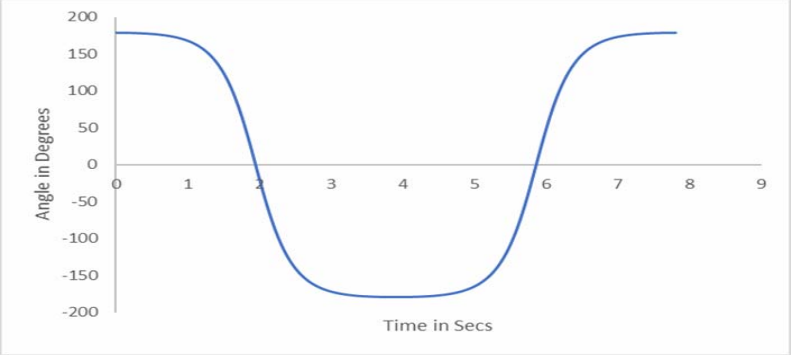

Fig. 2 – Finite element solution for motion profile at amplitude of 179°.

The profile of the present study is better than that in [1] as far as curve slope smoothness is concerned at θ = 0 as seen in Fig. 3. It should be noted that in [1] the period was calculated from numerical integration and had a value of 7.35 s while the period from the power series solution is 7.806 s at the amplitude of 179°. [1] used then numerical integration to compute the motion profile where θ was assumed and the corresponding time was accordingly calculated. However, all profiles in [1] are smooth up to amplitude of 170°. The FEM motion profile when using the boundary conditions as by Eq. (11b) is indistinguishable from that in Fig. 2. The computed amplitude at the end of the time period in that case was 179.0025° which is very close to the expected value of 179°.

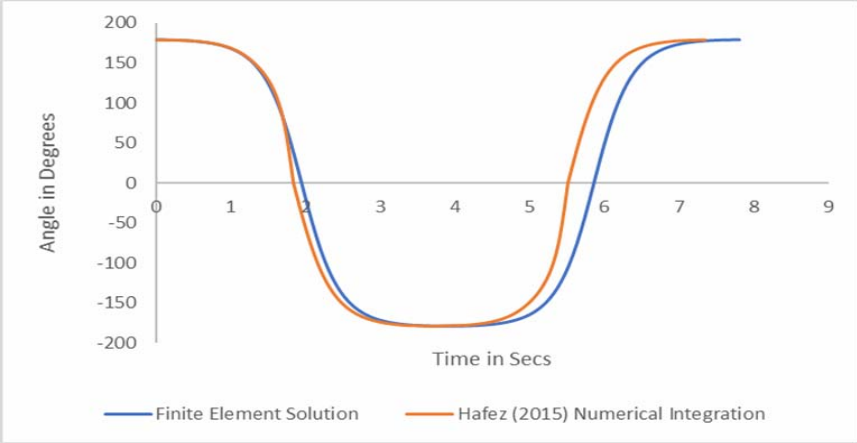

Fig. 3 – Comparison between FEM current solution and numerical integration solution.

It is noted that when the domain length is taken equal to two-period length the FEM numerical solution produces automatically two cycles as shown in Fig. 4. The computed amplitude and frequency in the second cycle are equal to their counterparts in the first cycle signaling nonexistence of numerical dissipation or numerical damping, i.e. achieving numerical stability. In fact more than two cycles were obtained without numerical damping.

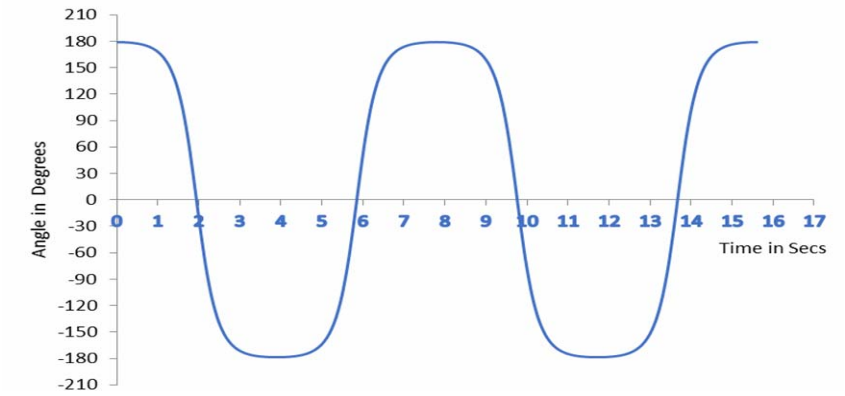

Fig. 4 – Motion profile at amplitude of 179º for two complete cycles.

Figure 5 shows the velocity profile for one cycle which is conforming to that of [6] and [1]. As expected from the physics of motion, the computed velocity magnitude is maximum with magnitude of 6.26 m/s at the one-fourth and three-fourths of the period corresponding to the bob at $\theta = 0$. The velocity profile does not exhibit the harmonic pattern which is seen at small amplitudes. Nonlinearity is at its maximum at this very high amplitude of 179°.

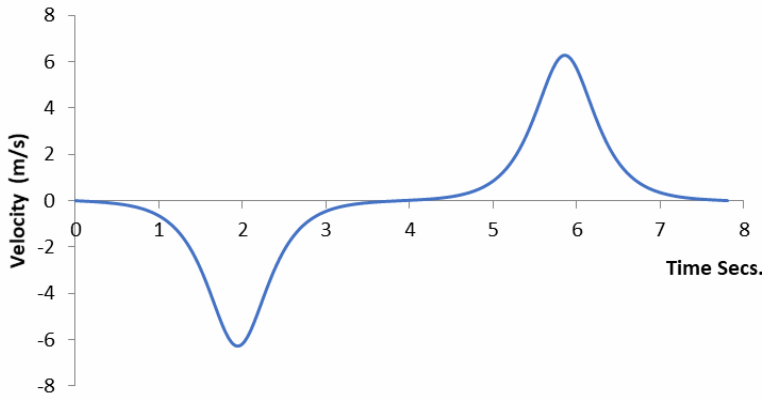

Fig. 5 – Velocity profile at amplitude of 179° for one cycle.

Figure 6 shows the energy profiles conforming also to [11] (amplitude was 170°) and [1]. In addition the sum of the potential and kinetic energies is constant throughout the period, indicating conservation of the total energy. The pendulum mass was taken as 0.5 kg (the mass does not affect pendulum motion) and its length was 1.0 m. Interestingly, the potential energy time intervals at which the maximum value is equal to the total energy are longer than those of the kinetic energy as exemplified by the long- plateau intervals in Fig. 6.

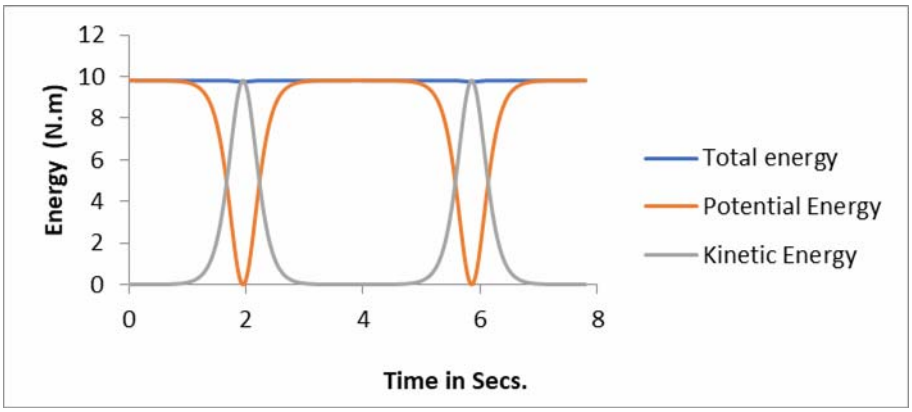

Fig. 6 – Total, potential and kinetic energies at amplitude of 179° for one cycle.

Figure 7 shows the motion profile at an intermediate regimes such as at amplitude $\theta = 90°$ along with that of the linear model solution which was given by Eq. (3). Clearly, at such amplitude deviations occur between the nonlinear and linear models. The FEM nonlinear profile coincides with the numerical integration solution by [1]. The two periods calculated from the power series and numerical integration by [1] are equal at this amplitude.

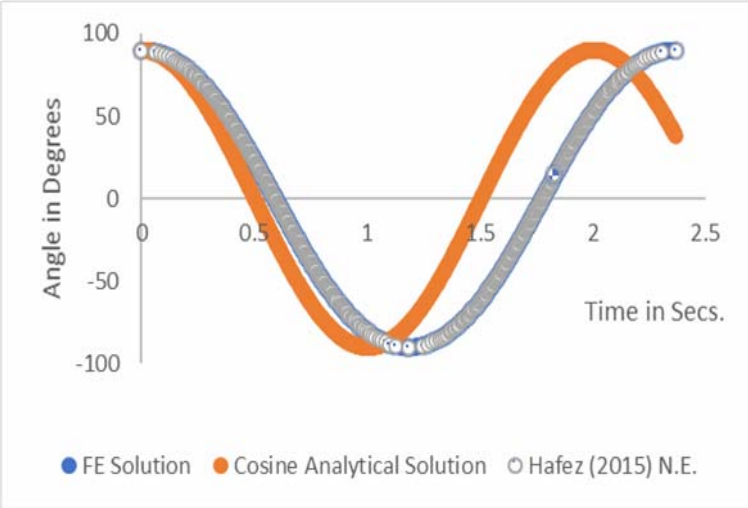

Fig. 7 – Profile motion for amplitude of 90°.

The two velocity profiles from the FEM and numerical integration are also coinciding as seen in Fig. 8.

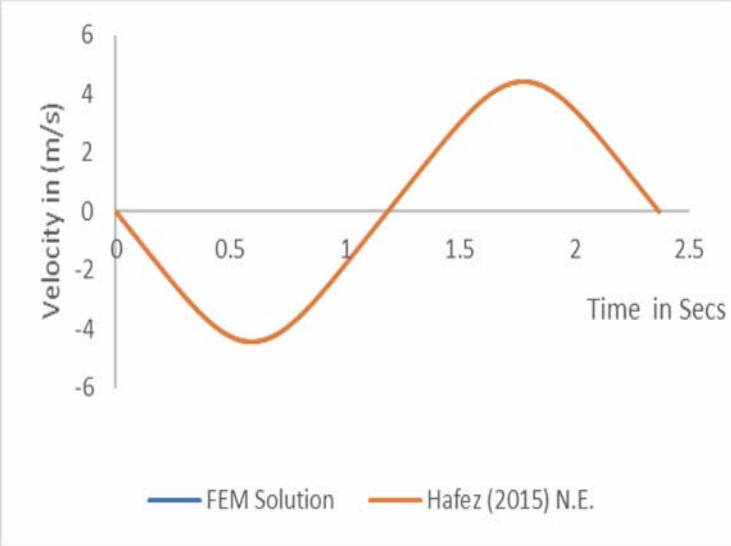

Fig. 8 –Velocity profile at amplitude of 90°.

The energy profiles shown in Fig. 9, which are computed by the FEM, matched those in [1] and exhibit conservation of energy.

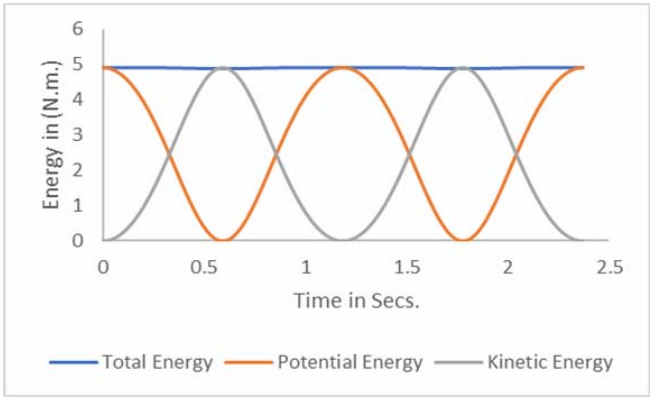

Fig. 9 – Energy profiles at amplitude of 90°.

Figures 10, 11, and 12 show the FEM computed motion, velocity and energy profiles, respectively at amplitude of 14°. The finite element solution for θ matches that of the linear analytic solution.

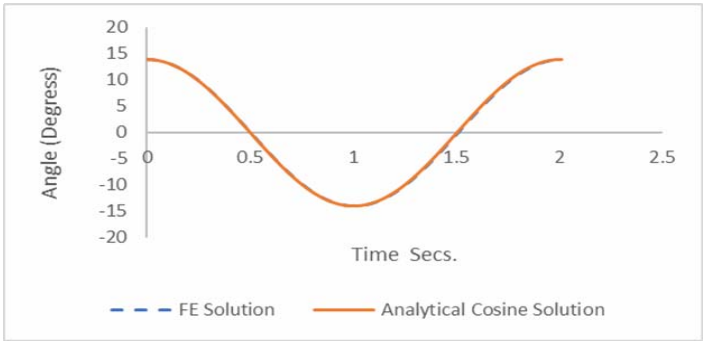

Fig. 10 – Motion profile at amplitude of 14°.

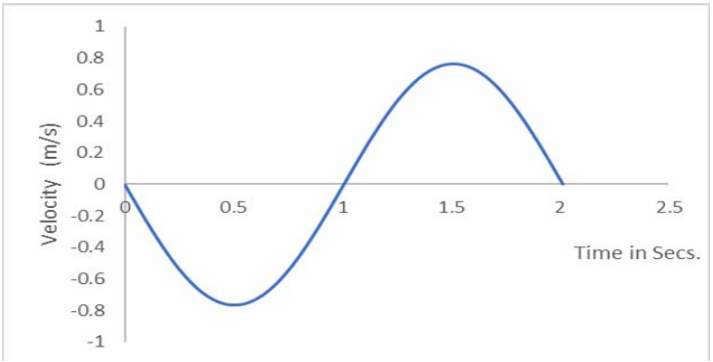

Fig. 11 – Velocity profile at amplitude of 14º.

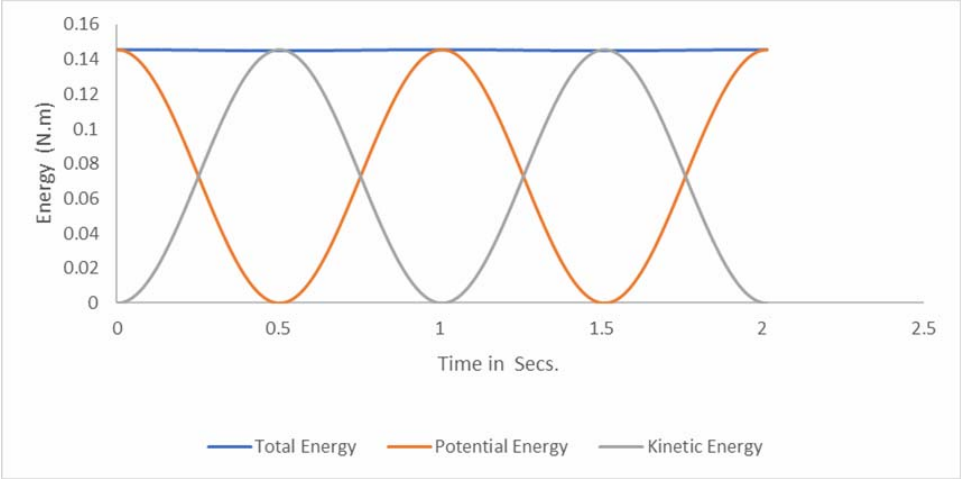

Fig. 12 – Total, potential and kinetic energy profile at amplitude of 14°.

Figures 13 and 14 show the FEM computed motion profiles for various amplitudes which can be useful to mathematicians, physicist and engineers.

Besides, the success of the methods and techniques used in this work encourages the beginning for using numerical methods in further investigations of the nonlinear pendulum under damped oscillations due to frictional and resistance forces as is seen in the following sections.

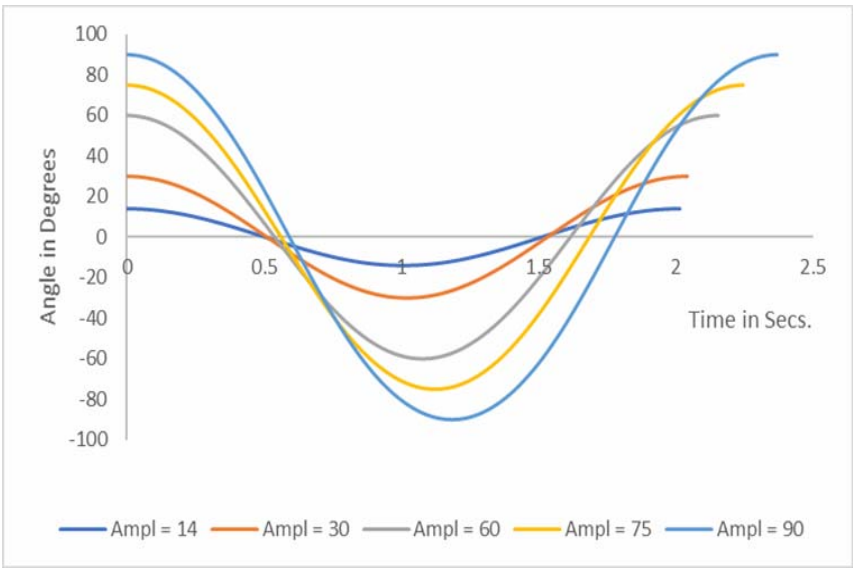

Fig. 13 – FEM computed motion profiles for amplitudes up to 90°.

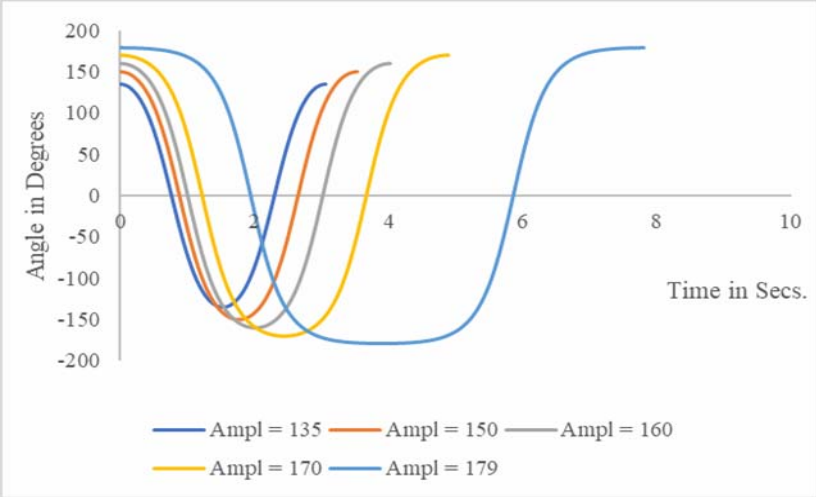

Fig. 14 – FEM computed motion profiles for amplitudes from 135º to 179º.

6. DAMPED OSCILLATIONS DUE TO FRICTION

The subject of damped pendulum motion is very important in vibration mechanics and earthquake engineering. Damped motion could be due to forces opposite to the direction of motion. In the modeling process resistance to motion by forces such as friction could be assumed proportional to the velocity [2]. In this case the pendulum governing equation becomes:

$$m\theta''(t) + c\theta'(t) + \frac{mg}{L}\sin\theta(t) = 0\,, \tag{17}$$

where c is the damping constant. Equation (17) for small θ (e.g. θ ≤ 14°), where $\sin\theta \approx \theta$ has the following analytical solution [12]:

$$\theta(t) = \theta_o \frac{-c}{e^{2m}} t\left(\cos(ht) + \frac{c}{2mh}\sin(ht)\right), \tag{18}$$

where $h = \sqrt{\frac{p^2}{m} - \frac{c^3}{4m^2}}$ and $p = \sqrt{\frac{mg}{L}}$.

The FEM model for undamped motion which was described earlier was modified to include the damping force while using Maclaurin Series for sin θ. The boundary conditions are slightly modified to be as $\theta(0) = \theta_0$ and $\theta'(\mathrm{TD}) = 0$ where TD is the length of the time domain taken as suitable multiples of the period. After a period of time equal to TD it is assumed that velocity is approaching zero.

Figures 15 and 16 for c values of 1.0 and 4.0 respectively, show comparison between the FEM nonlinear model with the analytical solution from Eq. (18) which was based on the linear model at amplitude = 20°. The values taken for the other parameters are that m = 1 kg, g = 9.81 m^2/s, and L = 0.1 m. It is clear that with increasing the value of the damping constant c, the quicker the dampening of the oscillations of the pendulum. For that amplitude with small value the nonlinearity is not expected to cause significant differences and the close match between the FE and the analytical solution suggests the success of predicting the damped pendulum motion.

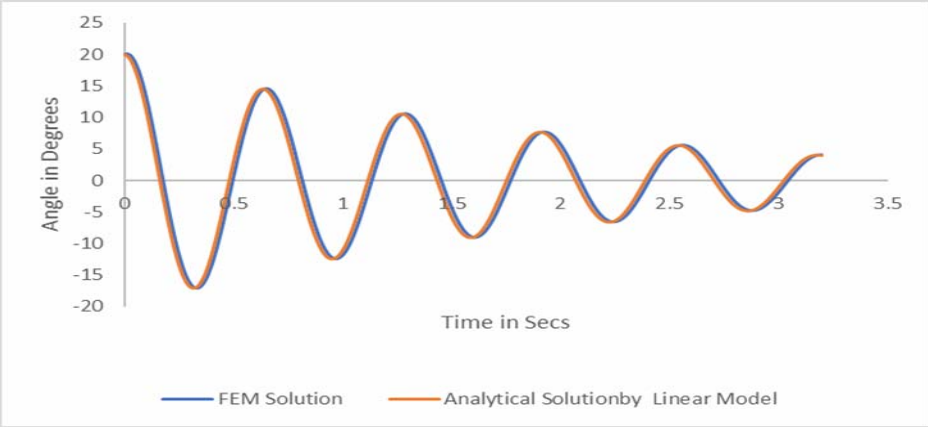

Fig. 15 – Comparison between the FEM and the analytical solution for pendulum with damped motion for damping constant c = 1.0.

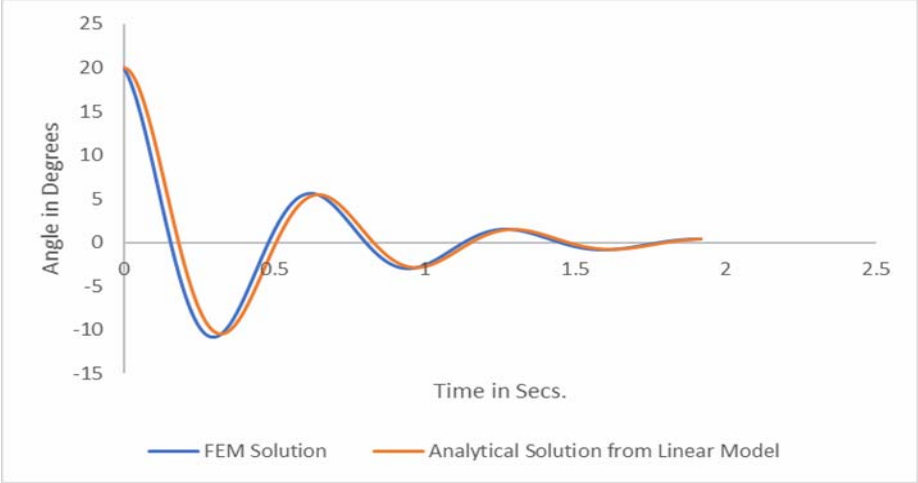

Fig. 16 – Comparison between the FEM and the analytical solution for pendulum with damped motion for damping constant c = 4.0.

7. DAMPED OSCILLATIONS DUE TO FRICTION AND DRAG RESISTENCE FORCES

When a body moves inside a fluid medium it is subjected to a drag force. For the pendulum moving in a fluid the drag force is given as by the third term of the following equation

$$mL\theta''(t) + cL\theta'(t) + C_D \rho A_p \frac{L^2}{2} \left|\theta'(t)\right| \theta'(t) + mg \sin\theta(t) = 0 , \tag{19}$$

where C_D is the drag coefficient, ρ is the fluid density, and A_p is the projected area of the pendulum body to the direction of motion. It is noted that the absolute value in Eq. (19) is used to ensure that the drag resistance force is in the opposite direction to the motion. Equation 19 includes two types of resistance to motion; namely; frictional resistance and form drag resistance. As in the last case, after a period of time equal to the length of the time domain (which is taken sufficiently long enough) it is assumed that velocity is approaching zero.

A simulation is run using the FEM model developed herein where it is assumed that the pendulum is moving in water where ρ = 1 000 kg/m^3, C_D is arbitrarily assumed as 1.5, $A_p = \pi d^2 / 4$ for a spherical pendulum (projected area becomes area of a circle) and d is the diameter of the bob. Figure 17 shows the FEM computed motion profile for an assumed data with: amplitude of 20°, m = 1 kg, g = 9.81 m^2/s, L = 0.1 m, d = 0.05 m and c is taken as zero to investigate resistance due to only form drag.

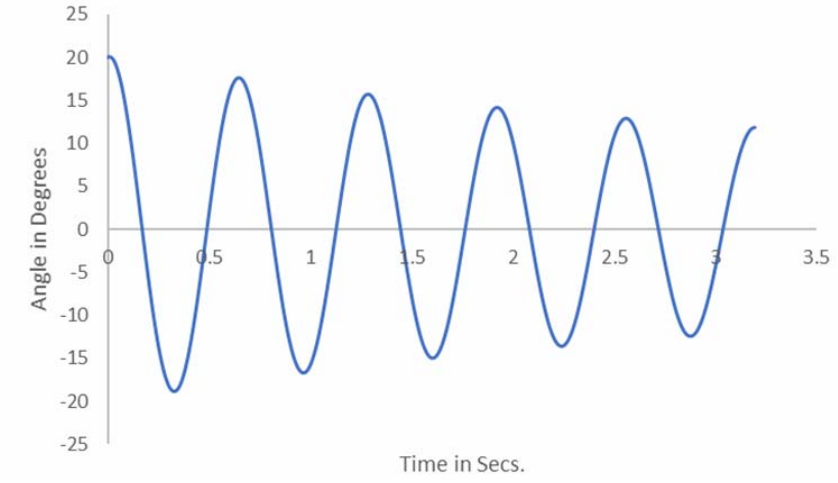

Fig. 17 – FEM computed motion profile for a pendulum moving in water with drag resistance.

Figures 18 and 19 show the corresponding velocity and energy profiles.

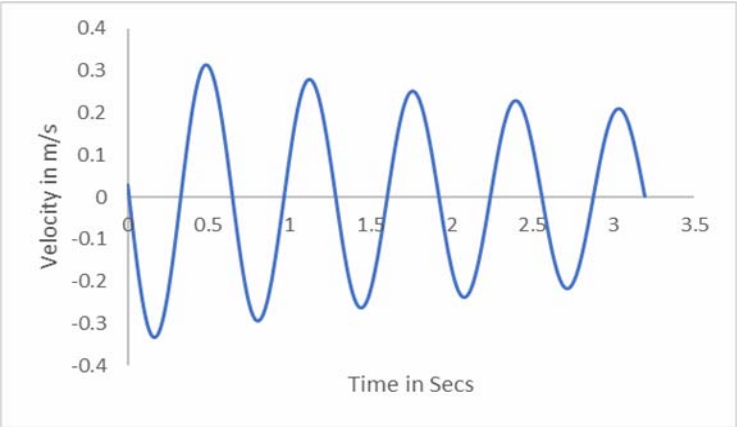

Fig. 18 – FEM computed velocity profile for a pendulum moving in water with drag resistance.

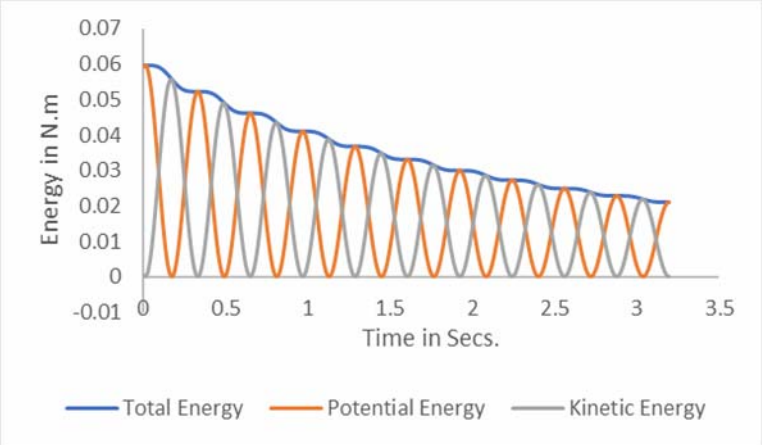

Fig. 19 – FEM computed energy profiles for a pendulum moving in water with drag resistance.

Figure 20 shows three FEM computed angle profiles where the first considers only the drag force resistance by water on the pendulum bob ($c = 0$), the second considers the form drag and frictional resistance forces acting together with $c = 1$ while the third considers the form drag and frictional resistance together with $c = 4$. It is clear that with increasing the value of the damping coefficient c, the damping of the oscillations accelerates. Similarly with increase in the drag coefficient the effect of damping is felt much more. This study should open the floor now to future numerical investigations of other complex pendulum types.

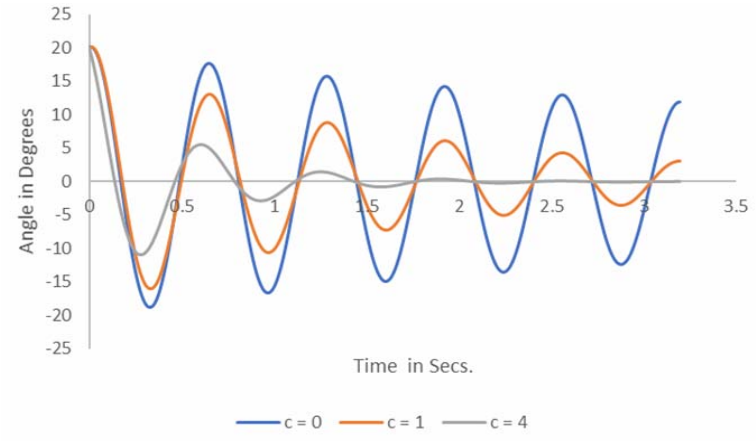

Fig. 20 – Effects of frictional and drag resistances on a pendulum moving in water.

8. DISCUSSION

The success of the developed approach and the Finite Element model for solving the nonlinear pendulum equation, preludes to important implications and paves the way for tackling other types of differential equations with similar nature. For example, if the sine of the displacement angle term is replaced by a cosine or tangent of the displacement angle, the same methodology applies by using the Maclaurin series expansion for the cosine or tangent function respectively. Several functions have a well-known Maclaurin series expansion such as: e^{θ}, $\ln(1+\theta)$, $\tan^{-1}(\theta)$, $\sinh(\theta)$, and $\cosh(\theta)$ as seen in [13]. Such functions of the unknown variable will cause nonlinearity of the differential equation and the proposed technique here can be used to overcome the nonlinearity.

As an example consider a pendulum under the influence of a horizontal force which could be electromagnetic force which is termed as Fe. In such case the governing equation of the pendulum motion assuming for the moment that no resistance forces exist, becomes:

$$ml\theta''(t) + mg\sin\theta(t) + F_e\cos\theta(t) = 0\,. \tag{20}$$

Equation (20) could be written as:

$$\theta''(t) + \frac{g}{L}\sin\theta(t) + \frac{F_e}{mL}\cos\theta(t) = 0\,. \tag{21}$$

Now using the Maclaurin's series expansion for the sine and cosine functions in Eq. (21) to obtain:

$$\theta''(t)+\frac{g}{L}\sum_{n=0}^{\infty}(-1)^{n}\frac{\theta^{2n+1}}{(2n+1)!}+\frac{F_e}{mL}\sum_{n=0}^{\infty}(-1)^{n}\frac{\theta^{2n}}{(2n)!}=0. \tag{22}$$

Equation (22) is subject to boundary conditions depending on the nature of the problem at hand. The electromagnetic force could be periodic or constant in time.

9. CONCLUSIONS

The nonlinear pendulum initial value problem could be converted into a two-point boundary value problem. This is possible owing to power series solution that determines explicit expression of the period of motion in terms of the initial displacement angle (amplitude). In this way the time of motion which is given by the period of motion is considered as a space domain. The periodic nature of the pendulum problem allows specifying the amplitude value at the two ends of the domain as the two end boundary conditions. Using Maclaurin's power series representation for the sine function in the pendulum differential equation with ten terms (powers up to the 19^{th} power) proved very successful in obtaining solutions up to initial angle displacement of 179°. Imposing the boundary conditions in increments facilitated overcoming the high nonlinearity and obtaining good initial guessing solution needed for the iterative solution process. The Finite Element method, which is the crown of existing numerical methods, was successful in solving the nonlinear simple pendulum problem. Nine Gauss quadrature points were sufficient for integrating the element matrices. Newton-Raphson technique for solving nonlinear algebraic set of equations proved its sufficiency and efficiency too. The ability to solve the differential equation form of the nonlinear simple pendulum allows ease in dealing with tangential forces to the pendulum bob's direction of motion such as the resistance and electromagnetic forces. The present approach succeeded in predicting the pendulum motion profile under damped conditions due to resistance forces such as friction and fluid resistance forces (form drag). The present approach furnishes the floor for tackling more general pendulum problems where forces like electromagnetic forces exist.

Received on November 6, 2021

REFERENCES

1. HAFEZ, Y., *Complete analysis of the nonlinear pendulum for amplitudes in all regimes using numerical integration*, International Journal of Numerical Methods and Applications, **14**, *1*, pp. 53–76, 2015.
2. EDWARDS, C.H., PENNY, D.E., *Elementary differential equations with boundary value problems*, Sixth Edition, Pearson International Edition, 2009, pp. 137, 533–537.

3. FULCHER, L.P., DAVIS, B.F., *Theoretical and experimental study of the motion of the simple pendulum*, Am. J. Phys., **44**, *1*, pp. 51–55, 1976.
4. BENACKA, J., *Power series solution to the pendulum equation*, International Journal of Mathematical Education in Science and Technology, **40**, *8*, pp. 1109–1117, 2009.
5. BELENDEZ, A., PASCUAL, C., MENDEZ, D.I., BELENDEZ, T., NEIPP, C., *Exact solution for the nonlinear pendulum*, Revista Brasileira de Ensino de Fisica, **29**, *4*, pp. 645–648, 2007.
6. OCHS, K., *A comprehensive analytical solution of the nonlinear pendulum*, Eur. J. Phys., **32**, *2*, pp. 479–490, 2011.
7. BELENDEZ, A., ARRIBAS, E., ORTUNO, M., GALLEGO, S., MARQUEZ, A., PASCUAL, I., *Approximate solutions for the nonlinear pendulum equation using a rational harmonic representation*, Computers and Mathematics with Applications, **64**, *6*, pp. 1602–1611, 2012.
8. SINGH, I., ARUN, P., LIMA, F., *Fourier analysis of nonlinear pendulum oscillation*, Revista Brasileira de Ensino de Fisica, **40**, *1*, e1305, 2018.
9. THOMPSON, E.G., *Introduction to the finite element method, theory, programming, and applications*, Fifth ed., John Wiley &Sons, Inc., 2005.
10. BURDEN, R.L., FAIRES, J.D., *Numerical Analysis*, Third Edition, PWS Publishers, pp.184–188, 1985.
11. BUTIKOV, I. E, *The rigid pendulum – An antique but evergreen physical model*, European Journal of Physics, **20**, *6*, 2003.
12. NRICh maths, Considering the simple pendulum with friction,
https://nrich.maths.org/content/id/.../Paulnot%20so%20simple%20pendulum%202.pd..
13. SWOKOWSKI, E.W., OLINICK, M., COLE, J.A., *Calculus*, Sixth Edition, PWS Publishing Company, Boston, USA, 1994.